Mitigation of Sub-synchronous Oscillation Caused by Thyristor Controlled Series Capacitor Using Supplementary Excitation Damping Controller

Xi Wu*, Ping Jiang*, Bo-lin Chen*, and Hua-chuan Xiong*

Abstract –The Test Signal Method is adopted to analyze the impact of thyristor controlled series capacitor (TCSC) on sub-synchronous oscillation. The results show that the simulation system takes the risk of Sub-synchronous Oscillation (SSO) while the TCSC is operating in the capacitive region. A supplementary excitation damping controller (SEDC) is used to mitigate SSO caused by the TCSC. A new optimization method which is aimed for optimal phase compensation is proposed. This method is realized by using the particle swarm optimization (PSO) algorithm. The simulation results show that the SEDC designed by this method has superior suitability, and that the secure operation scope of the TCSC is greatly increased.

Keywords: Sub-synchronous oscillation (SSO); Supplementary excitation damping controller (SEDC); Thyristor controlled series capacitor(TCSC); Particle swarm optimization (PSO)

1. Introduction

Sub-synchronous oscillation (SSO) is an electric power system condition where the electric network exchanges significant energy with a turbine-generator at one or more of the natural frequencies of the combined system below the synchronous frequency of the system following a disturbance from equilibrium[1-2].

The impact of a Thyristor Controlled Series Capacitor (TCSC) on SSO got broad attention from numerous experts and scholars[3-6].In [3], The frequency response of a TCSC device was obtained through a frequency scanning technique (FSM). It was observed that the TCSC operating under constant impedance control, with a nominal firing angle, is inductive in the subsynchronous resonance (SSR) frequency range. However, if the steady-state operation results in higher firing angles, the risk of tuning unstable torsional interactions is increased because the device becomes capacitive in the SSR frequency range. It is demonstrated by [4, 5] that TCSC shows capacitive characteristics at fundamental frequency while it shows inductive characteristics at subsynchronous frequency if the firing angle decrease to a certain value. Zhang and Xu [6] studied the SSR damping characteristics with TCSC and the results show that the conducting angle of the thyristor has a great influence on the damping of the TCSC, and that the larger the conducting angle gets, the greater the TCSC reduces the electrical negative damping around the resonant point. In sumnation, the impacts of TCSC on SSO are different under different operating states; sometimes a TCSC may even increase the risk of SSO.

TCSC can control the degree of series compensation consistently, and therefore it changes sub-synchronous conditions. As well, the band width of the harmonics created by TCSC is wide enough to allow signals of sub-synchronous resonance frequency to pass. This could excite sub-synchronous resonance under certain conditions. However, the mitigation of SSO caused by TCSC has rarely been presented. In this paper, the impact of TCSC on SSO is studied by the complex torque approach based on time domain simulation. A Supplementary excitation damping controller (SEDC) is used to mitigate SSO caused by TCSC. The optimization method based on the Particle Swarm Optimization (PSO) algorithm is also proposed in this paper.

The organization of this paper is as follows: In Section 2, the impact of TCSC on SSO is studied. In Section 3, the structure and principle of SEDC is introduced. In Section 4, the optimization method for SEDC is proposed. The time domain simulation results are displayed in Section 5. In Section 6, conclusions are duly drawn.

2. The Impact of TCSC on SSO

2.1 The Complex Torque Coefficient Method

* School of Electrical Engineering, Southeast University, China. (wuxi112233@163.com)

Received 28 June 2011; Accepted 01 November 2011

The terminology of the complex torque coefficient is proposed by I.M. Canay [7]. The synchronous complex torque coefficients are defined as follows:

$$\dot{K}_e(j\lambda) = \Delta\dot{T}_e / \Delta\dot{\delta} = K_e(\lambda) + j\lambda D_e(\lambda) \quad (1)$$

$$\dot{K}_m(j\lambda) = \Delta\dot{T}_m / \Delta\dot{\delta} = K_m(\lambda) + j\lambda D_m(\lambda) \quad (2)$$

Here K_e and D_e represent the electrical spring coefficient and the electrical damping coefficient respectively; K_m and D_m represent the mechanical spring coefficient and the mechanical damping coefficient respectively. $\lambda = f_r / f_n$, where fr is the subsynchronous frequency, and fn is the base frequency.

The system is assumed to be stable if the net damping at any torsional-mode frequency is positive.

$$\sum D(\lambda) = D_e(\lambda) + D_m(\lambda) > 0 \quad (3)$$

The mechanical damping torque coefficient can be achieved by frequency-scanning [7]. The electrical damping coefficient can be found through the Test Signal Method[8]. The related expression is:

$$D_e(f) = \mathrm{Re}\left(\frac{\Delta\dot{T}_e(f)}{\Delta\dot{\omega}(f)}\right) \quad (4)$$

where $D_e(f)$ is the electrical damping torque coefficient of the unit in per unit, $\Delta\dot{T}_e(f)$ is the vector of the increments of the electromagnetic power of the generator in per unit, and $\Delta\dot{\omega}(f)$ is the vector of the increments of the angular velocity of the rotor in per unit when a ripple torque with frequency f is imposed on the rotor.

2.2 The studied system

The First IEEE Benchmark [9] model is adopted, including a TCSC device which replaces the fixed series capacitor. The parameters of the TCSC is set as C=25.464μF, L=0.0442H, k=$\sqrt{X_C / X_L}$ =2.5. Fig.1 shows the network of the studied system. A 892.4 MVA synchronous generator is connected to an infinite bus via a highly compensated 500 kV transmission line. The mechanical system consists of a four-stage steam turbine, the generator and a rotating exciter, the shaft nature frequencies are 15.71Hz, 20.21Hz, 25.55 Hz, 32.28 Hz and 47.46Hz. In this paper, we set damping factors D1= D2= D3= D4= D5= D6=0.01,D12= D23= D34= D45= D56= 0.

2.3 Damping analysis

The negative mechanical damping characteristic achieved through frequency-scanning is shown in Fig 2.

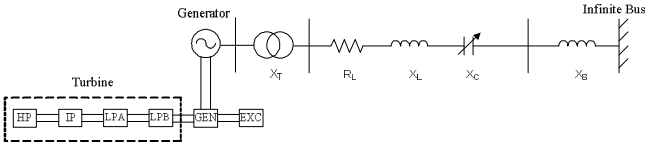

Fig. 1. The network of the studied system.

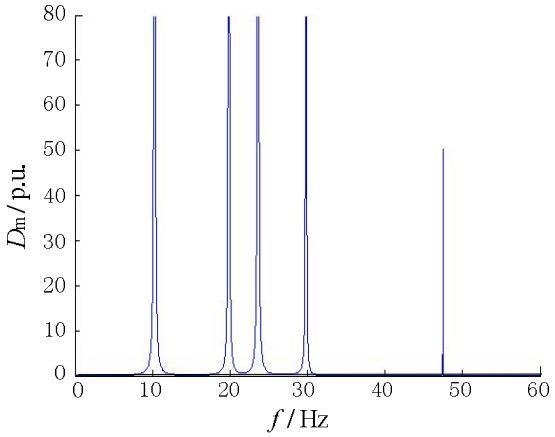

Fig. 2. The negative mechanical damping characteristic.

The damping coefficients of the shaft nature frequencies are shown in Table 1.

Table 1. Damping coefficients of the shaft nature frequencies

Mode	Frequency (Hz)	Damping coefficient (p.u.)
Torsional 1	15.71	0.159
Torsional 2	20.21	7.351
Torsional 3	25.55	0.460
Torsional 4	32.28	0.066
Torsional 5	47.46	50.35

Here we define some related angles of the TCSC. We define α as the firing delay angle measured from the positive zero crossing or the negative zero crossing of the capacitor voltage, β as the firing leading angle, $\beta = 180° - \alpha$, σ is the conducting angle. In steady state, $\sigma = 2\beta$. The electrical damping characteristic when TCSC operates in the inductive region is shown in Fig.3, the conducting angle of TCSC is set to 140°, 150°, 160° and 170° respectively. It is clearly depicted that the negative electrical damping at every SSO frequencies is very small, and the system is stable. Fig.4 shows the electrical damping characteristic when TCSC operates in the capacitive region with conducting angles set to 140°, 150°, 160° and 170°

respectively. It shows that significant negative damping exists in the sub-synchronous region. At some SSO frequencies, $D_e + D_m < 0$, the system has a risk of exciting SSO. As well, damping distribution and the resonant center also changes significantly as conducting angle of TCSC changes.

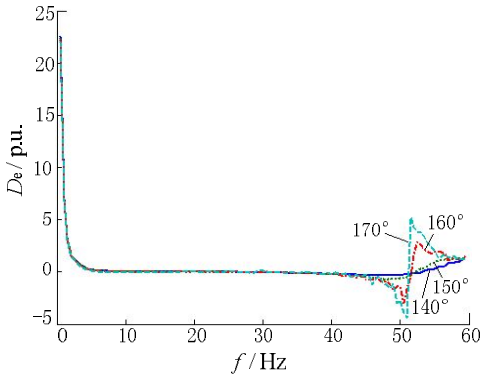

Fig. 3. The electrical damping characteristic when TCSC operates in the inductive region.

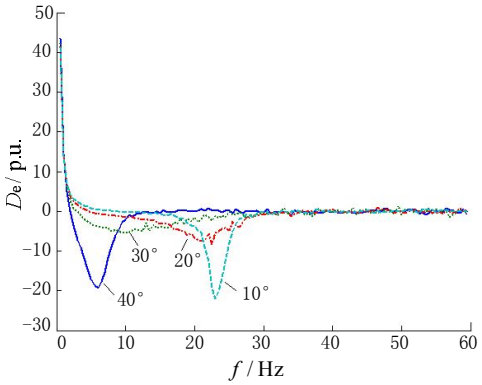

Fig. 4. The electrical damping characteristic whenTCSC operates in the capacitive region.

3. Structure and Mechanism of the SEDC

SEDC is a real-time control system that works through the excitation system by modulating the field voltage at the torsional frequencies.[10-12] Fig. 5 shows the block diagram of the SEDC.

The input signal of SEDC is delta mechanical speed, which after proper filtering and conditioning becomes the standard signal $\Delta\omega$. It is then passed through a band-pass filter tuned to a specific mode. The filtered output is subsequently amplified and phase-shifted with the gain Gk and unity-gain phase-shifter $((1+T_{ib}s)/(1+T_{ia}s))^2$ becoming the control signal for the corresponding mode. Finally, the summed signal of all torsional modes is clipped and added to the automatic voltage regulator to modulate the field voltage.

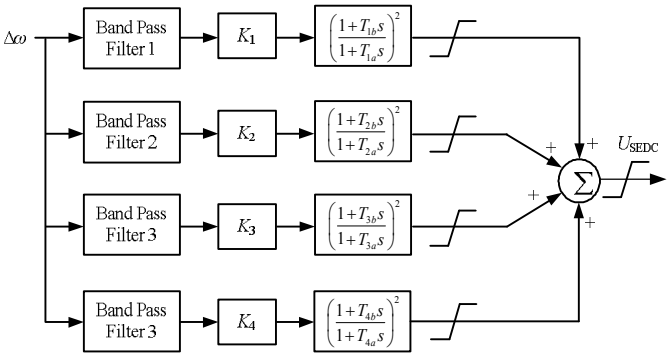

Fig. 5. Block diagram of the SEDC.

Fig. 6 shows the relationships between Shaft speed deviation $\Delta\omega$, the additional torque $\Delta T_e'$ provided by EDC and the damping torque $\Delta T_D'$. At the same angular frequency, if the angle between $\Delta\omega$ and $\Delta T_e'$ is less than 90°, the additional damping torque $\Delta T_D'$ is positive. Positive damping torque $\Delta T_D'$ is helpful in suppressing SSO.

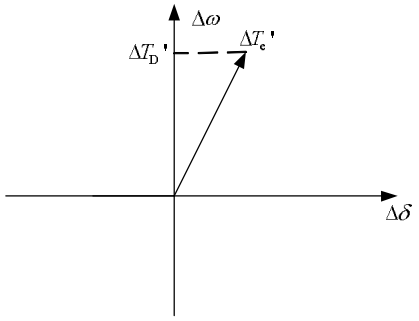

Fig. 6. Vector diagram of Δδ, Δω, ΔT_e' and ΔT_D'.

4. Using SEDC to Suppress SSO Caused by TCSC

According to section 2, the studied system is stable when TCSC operates in the inductive region. However, the system has a risk of exciting SSO when TCSC operates in the inductive region. Moreover, damping distribution changes significantly with the conducting angle of the TCSC. So the SEDC needs to provide damping over a wide range of operating conditions. In this paper, we aimed for optimal phase compensation. To obtain the phase lag of the system at different operating states, a series of small oscillating signals at 15.71Hz, 20.21Hz, 25.55 Hz, 32.28 Hz are added to the Voltage Reference(U_{ref}) of the AVR, and the delta electromagnetic torque ΔT_e is obtained when the simulation reaches a steady state. The Fourier resolution of ΔT_e, and $\sum\Delta U_s$ is performed to obtain $\Delta T_e(jf)$, $\sum\Delta U_s(jf)$ in different frequencies. The phase lag (θ_{lag}) between the exciter input and the electrical torque can be calculated by:

$$\theta_{\text{lag}}(f) = \text{Im}(\frac{\Delta T_e(jf)}{\Delta U_s(jf)}) \quad (5)$$

Table 2. Phase lags of the system at different operating states

Conducting angle of TCSC	Frequency (Hz)			
	15.71	20.21	25.55	32.38
40°	-172.1°	-168.6°	-164.7°	-162.5°
30°	-160.9°	-172.4°	-177.3°	-177.0°
20°	-132.8°	-155.3°	-194.8°	-194.3°
10°	-121.6°	-119.7°	-222.7°	-209.2°

Table 2 gives the phase lag angles at the torsional frequency when TCSC opreates with the conducting angle set to 10°, 20°, 30° and 40° respectively. Aiming for the best phase compensation, the task of control-design can be formulated into the constrained nonlinear optimization problem:

$$\begin{cases} \min f = \sum_{i=1}^{4}\sum_{j=1}^{4} W_{ij}(\theta_{ij} - 2\times \text{Im}\left(\frac{1+T_{ib}\times j\omega_i}{1+T_{ia}\times j\omega_i}\right))\text{^}2 \\ W_{ij} = \mid D_{\text{m}ij} + D_{\text{e}ij} \mid, \quad \text{if } D_{\text{m}ij} + D_{\text{e}ij} < 0 \text{ ; else } W_{ij} = 0 \\ 0.1 \le T \le 1 \end{cases} \quad (6)$$

where T_{ia}, T_{ib} (i=1,2,3,4) are the control parameters to be optimized, which represent the time constant of the phase-shifter block for the i-th torsional mode; ω_i is the angular velocity of the i-th mode; W_{ii} is the positive weight coefficient for the i-th mode under the j-th operating condition; $D_{\text{m}ii}$ and $D_{\text{e}ii}$ are the mechanical damping coefficient and the electrical damping coefficient of the the i-th mode under the j-th operating condition respectively; θ_{ij} is the phase need to be compensated by SEDC at the i-th mode frequency under the j-th operating condition, it can be obtained by:

$$\begin{cases} \theta_{ij} = -\theta_{lagij}, \quad \text{if } \theta_{lagij} > -90 \\ \text{else } \theta_{ij} = -180 - \theta_{lagij}, \quad \text{if } -270 < \theta_{lagij} < -90 \\ \text{else } \theta_{ij} = -360 - \theta_{lagij}, \quad \text{if } \theta_{lagij} < -270 \end{cases} \quad (7)$$

Where θ_{lagij} is the the phase lag between the exciter input and the electrical torque which shown in Table II;

To solve the control-design problem (6), which is a complex nonlinear optimization problem, we use the Particle swarm optimization (PSO) algorithm.

PSO is a form of evolutionary computation technique (a search method based on natural systems) developed by Kennedy and Eberhart [13]. This technique uses a population of particles to swarm through the design space with specified velocities. The population of agents or particles tries to simulate their social behavior in the problem space and arrives at an optimum value of fitness function. The key advantages of PSO over the other optimization techniques are as follows: a lower sensitivity to the nature of the objective function, a derivative free property unlike many conventional techniques, easy implementation and etc[14].

The eight parameters (T_{1a}, T_{1b}, T_{2a}, T_{2b}, T_{3a}, T_{3b}, T_{4a}, T_{4b}) to be optimized are real coded in a particle. The algorithm starts with N particles. Each particle represents a candidate solution to the problem, which has a current position, x_k (k=1,2,…N) and a current velocity v_k , in the search space. The value of each particle is determined by fitness function (6). The previous best value is called the pbest of the particle and is represented as p_k. Thus, p_{k} is related only to a particular particle k. The best value of all the particles' pbests in the swarm is called the gbest and is represented as p_{g}. The following steps explain the procedure in the optimization method for the SEDC.

(i) Initialize a population of particles with random positions and velocities.

(ii) For each particle, evaluate the desired optimization fitness function, which has been introduced in (6).

(iii) Compare every particle's fitness evaluation with its pbest value (previous best value), p_{k}. If the current value is better than p_{k}^{n}, then set p_{k} value equal to the current value and the p_{k} location equal to the current location in an 8-dimensional space.

(iv) Compare the updated previous best values with the population's previous gbest value. If any of pbest values is better than p_{g}, then update p_{g} and its parameters.

(v) Compute the new velocities and positions of the particles according to (8) and (9) respectively.

$$v_i^{n+1} = w\times v_i^n + c_1\times r_1\times(p_i^n - x_i^n) + c_2\times r_2\times(p_g^n - x_i^n) \quad (8)$$

$$x_i^{n+1} = x_i^n + v_i^{n+1} \quad (9)$$

In these equations, super script (n+1) denotes (n+1)-th generation and super script n denotes n-th generation. w is called the inertia weight, which controls the exploration and exploitation of the search space. c_1 and c_2 are learning factors. r_1 and r_2 are independent uniform random numbers.

(vi) Repeat from step (ii) until a specified terminal condition is reached, usually a sufficiently good fitness or a maximum number of iterations.

The following PSO parameters have been chosen after running a number of trials: population size = 20; generation number = 50; inertia weight w = 0.73; learning factors c_1 = c_2 =1.5. In our case, it is discovered that the performance of GASA is not sensitive to these parameters.

The optimized SEDC phase-shifter parameters obtained by the PSO are listed as follows:

T_{1a} = 0.1833, T_{1b} = 0.9972, T_{2a} = 0.1366, T_{2b} = 0.8978,
T_{3a} = 0.9898, T_{3b} = 0.3307, T_{4a} = 0.6290, T_{4b} = 0.2440

After finishing phase-shifter parameters optimization, magnification parameters of the SEDC need to be adjusted in the simulation system until the SEDC can provide sufficient damping. The gains of the SEDC are set as:

$$K_1 = 50,\ K_2 = 120,\ K_3 = 0.9,\ K_4 = 1.$$

5. Simulation Results

The program PSCAD/EMTDC was adopted for simulation. The initial firing delay angle of the TCSC is set to α = 160°. A small shaft disturbance is introduced at t=11s, and the firing delay angle of the TCSC is adjusted at t=15s, t=20s, t=25s (the firing delay angle increases by 5° at each time point). The torque-time curves of shafting masses in the system without and with SEDC are shown in Fig.7 and Fig.8 respectively.

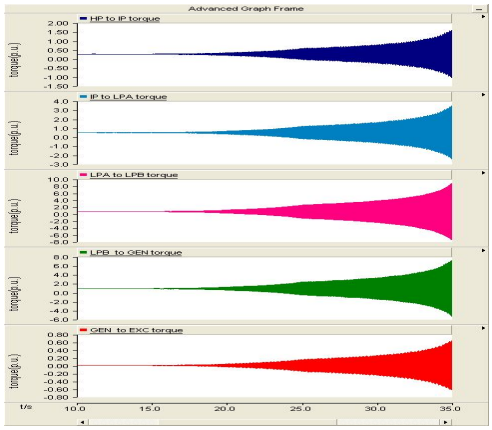

Fig.7. Torque-time curves of shafting masses in the system without the SEDC.

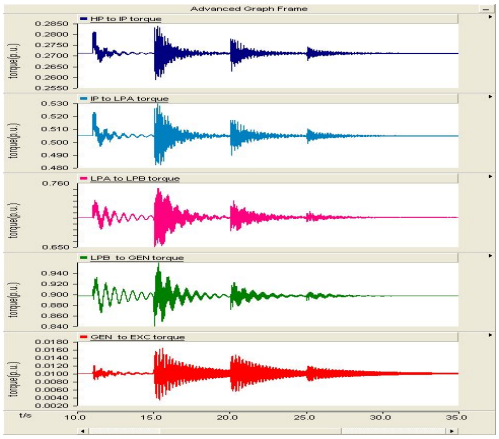

Fig.8. Torque-time curves of shafting masses in the system with SEDC.

According to Fig.7 and Fig.8, the SSO has been well suppressed and the secure operation scope of the TCSC is greatly increased by adding the SEDC to the testing system.

6. Conclusions

In this paper, the impact of TCSC on SSO is analyzed. Further, a new optimization method which is aimed for the optimal phase compensation is proposed. This method is realized by using the PSO algorithm. Conclusions can be drawn as follows:

(i) The studied system has a risk of exciting SSO when TCSC operates in the capacitive region.

(ii) Damping distribution and phase lag characteristic changes significantly with the conducting angle of TCSC.

(iii) The SEDC designed by this method has better suitability, and the secure operation scope of the TCSC is greatly increased.

Acknowledgements

The Authors are highly thankful for the financial support of project of the national eleventh-five year research program of China (2008BAA13B07) and innovation program for graduate students of Jiangsu province (CXZZ11_0151).

References

[1] IEEE Subsynchronous Resonance Working Group, "Terms, Definitions and symbols for subsynchronous oscillations,"*IEEE Trans. Power Appar. Syst.*, Vol.104, No. 6, pp. 1326-1334, Jun.1985.

[2] A. H. Nayfeh, A. Harb, C. M. Chin, A. M.A. Hamdan, L. Mili, "Bifurcation analysis of subsynchronous oscillations in power systems," *Elect. Power Syst. Res.,* Vol.47, No. 1, pp. 21-28, Oct.1998.

[3] L. A. S. Pilotto, A. Bianco, W. F. Long, A. A. Edris, "Impact of TCSC control methodologies on subsynchronous oscillations," *IEEE Trans. Power Deliv.*, Vol.18, No. 1, pp. 243-252,January 2003.

[4] R Hedin, V Henn, A H Johnson, "Advanced series compensation(ASC): Transient network analyzer studies compared with digital simulation studies," *in Proc. EPRI FACTS Conference*, Boston, 1992.

[5] N Christl, R Hedin, K Sadek, "Advanced series compensation (ASC) with thyristor controlled impedance," *in Proc. International Council on Large Electric Systems*, Paris, 1992.

[6] F. Zhang, Z. Xu. "SSR damping study on a generator connected to TCSC," in *Proc. IEEE PSCE'04*, New York, USA, 2004.

[7] I. M. Canay, "A novel approach to the torsional interaction and electrical damping of the synchronous machine part I: theory," *IEEE Transactions on PAS*, Vol.PAS-101, No.10, pp.3630-3638, Oct. 1982.

[8] Zheng Xu, Zhouyan Feng, "A novel unified approach for analysis of small-signal stability of power systems," In *proc. 2000 IEEE Power Engineering Society Winter Meeting,* Singapore, 2000, Vol. 2, pp. 963-967.

[9] IEEE subsynchronous resonance task force, "First benchmark model for computer simulation of subsynchronous resonance," *IEEE Trans. Power Apparatus and Systems*, Vol. PAS-96, No. 5, pp. 1565-1572, Sep.,1977.
[10] C. E. J. Bowler, D. H. Baker, N. M. Mincer, and P. R. Vandiveer, "Operation and test of the Navajo SSR protective equipment," *IEEE Trans. Power App. Syst.*, vol. PAS-97, pp. 1030–1035, Jul. 1978.
[11] Xiaorong Xie, Xijiu Guo, and Yingduo Han, "Mitigation of multimodal SSR using SEDC in the Shangdu series-compensated power system," *IEEE Trans. Magnetics*, Vol.26, No.1, pp. 384-391, February 2011.
[12] D. Zhang, X. Xie, S. Liu, and S. Zhang, "An intelligently optimized SEDC for multimodal SSR mitigation," *Elect. Power Syst. Res.*, vol. 7, pp. 1018–1024, Jul. 2009.
[13] J. Kennedy and R. Eberhart, "Particle swarm optimization," in *Proc. IEEE International Conf. on Neural Networks*, Perth, Australia. vol. 4, Dec 1995, pp. 1942–1948.
[14] M. R. Alrashidi, M. E. El-Hawary, "A survey of particle swarm optimization in electric systems," *IEEE Transaction on Evaluation Computation*, pp. 1–6, 2003.

Xi Wu received his B.S. degree in electrical engineering from Southeast University in 2008, where he is currently pursuing his Ph.D. degree. His research interests are power system dynamics and control.

Ping Jiang received his B.S. degree in electrical engineering from Southeast University in 1982, and his M.S. degre e in electrical engineering from PLA University of Science and Technology, and his Ph.D in electrical engineering from Southeast University. He is a Professor with Southeast University. His research interests are power system dynamics and FACTS.

Bo-lin Chen received his B.S. degree in electrical engineering from Southeast University in 2009. His research interests are power system dynamics and control.

Hua-chuan Xiong received his B.S. degree in electrical engineering from Southeast University in 2009. His research interests are power system dynamics and control.